Results in Optics 18 (2025) 100764

Contents lists available at ScienceDirect

Results in Optics

journal homepage: www.sciencedirect.com/journal/results-in-optics

Characterization of birefringent Bragg gratings waveguides inscribed with the Femtoprint device

M.Tunon de Lara [a,b], L.Amez Droz [b,c], K. Chah [a], P. Lambert [b], C. Collette [c,d], C. Caucheteur [a,*]

[a] Electromagnetism and Telecommunication Department, Université de Mons, Belgium
[b] TIPs Department, CP 165/67, Université Libre de Bruxelles, 50 av FD Roosevelt, B-1050 Brussels, Belgium
[c] Department of Aerospace and Mechanical Engineering, Université de Liège, Liège, Belgium
[d] BEAMS Department, CP 165/56, Université Libre de Bruxelles, 50 av FD Roosevelt, B-1050 Brussel, Belgium

ARTICLE INFO

Keywords:
Femtosecond laser
Birefringence
Waveguide
Bragg grating
Fused silica
Refractive index

ABSTRACT

Since their advent, femtosecond (fs) laser pulses have been effectively employed to create micro and nano structures within host materials, such as silica glass. Their application is of growing interest in the fields of photonics and optomechanics and numerous achievements have been obtained to date. The technology has matured to such a degree that automated production processes like the FemtoPrint machine are now commercially available. While dealing with such powerful tools, users need to optimize the energy per pulse and polarization state to create effective structures on purpose. Thereby, studying the effect of these parameters on the relative quality of the fs laser pulses-engineered structures is of prime importance and can bring assistance or even a useful methodology for the scientific community using this tool or an equivalent technique. In this study, our focus revolves around exploring the characteristics of optical waveguides and in-built Bragg gratings created with the Femtoprint process in a flat glass substrate to extract pertinent information regarding their physical and optical properties, such as dimensions, refractive index modulation and birefringence. To that aim, we rely on three advanced methodologies: Digital holographic Microscope (DHM) analysis, polarization-based spectral measurements and infrared camera imaging, respectively. This analysis reveals important findings about the actual implemented refractive index modulation. For the investigated pulse energy (130 nJ), repetition rate (1 MHz) and scanning speed of the fs laser pulses beam, we show that the refractive index modification in the waveguide determined by DHM analysis lies in the range of 10^{-3}. This value is the highest reported so far in waveguides at this relatively low energy and high repetition rate of the laser pulses. Besides, the Bragg grating inscribed in the waveguide shows a spectral separation between the Bragg modes (300 pm) corresponding to an effective birefringence of the waveguide of 1.36 10^{-4}. This value depends on the polarization of the writing beam with respect to the scanning direction.

1. Introduction

Fs laser pulses represent potent tools with diverse applications in the industrial realm (Malinauskas et al., 2016). A notable instance is their use in the micro-nano engineering of silica glass substrates (Wang et al., 2021); wherein a tightly-focused; high-powered laser beam is employed to intricately carve, perforate, and adorn the material (both at its surface and in the volume). This laser beam can be precisely focused to a minute spot, enabling non-linear modifications within an even smaller volume than the focal point. Traditional mechanical or chemical techniques lack the precision to achieve such fine results. Additionally, the ultra-short pulses of these lasers allow for meticulous energy control, thereby minimizing thermal damage and ensuring the production of high-quality incisions. Depending on the desired outcome, the focused laser beam can either be maneuvered across the glass in a predetermined pattern or concentrated at specific points to fashion apertures or pathways. Advanced computer software can govern this process to guarantee precision and reproducibility. Moreover, the utilization of multiple laser beam scans, each focused at distinct depths, can generate intricate three-dimensional structures (Gattass et al., 2008). This method; known as femtosecond laser-assisted chemical etching, presents a multitude of potential applications, including the creation of microfluidic channels and optical components (Bellouard et al., 2004). Extensive research has delved into the mechanisms underlying material modifications induced

* Corresponding author.
E-mail address: christophe.caucheteur@umons.ac.be (C. Caucheteur).

https://doi.org/10.1016/j.rio.2024.100764
Received 13 June 2024; Received in revised form 7 October 2024; Accepted 24 November 2024
Available online 28 November 2024

by focused femtosecond pulse lasers (Bellouard et al., 2004; Taylor et al., 2003; Bellouard, 2011). In the case of glass; three distinct material modifications can be achieved; contingent on the characteristics of the employed femtosecond pulse laser, such as pulse energy and duration, repetition rate, scanning speed, scanning direction, and polarization (Beresna et al., 2014; Hnatovsky et al., 2005; Tien et al., 1999; Joglekar et al., 2003). As energy density levels increase; silica glass undergoes various structural changes:

(1) Densification (Chah et al., 2013; Zhou et al., 2010): This results in localized; isotropic changes in the refractive index at the focal point, potentially leading to the creation of optical waveguides and Bragg gratings (Will et al., 2002; Canning et al., 2011).

(2) Nano-grating: This manifests as structural alterations in the material, typically forming alternating silica nanoplanes and nanochannels perpendicular to the incident polarization of the laser beam. At this level of modification the material becomes more prompt to chemical etching by using various solutions like Potassium Hydroxide (KOH) (Taylor et al., 2003; Kiyama et al., 2009); Hydrofluoric acid (HF) (Marcinkevičius et al., 2001) or Sodium Hydroxide (NaOH) (Casamenti et al., 2021). Hence; cavities and mechanical structures can be created (Hnatovsky et al., 2005).

(3) Direct ablation: This scenario involves a significant amplification of pulse energy, leading to the creation of voids within the exposed material sample (Gattass et al., 2008; Liu et al., 1997).

As mentioned previously, the localized change in the refractive index by focusing fs laser pulses in a transparent glass substrate can be exploited to create three-dimensional structures such as waveguides. These latter can be produced either by a single-scan or multi-scan of the laser beam in the bulk material (Pasaila et al., 2006; Li et al., 2022). The mechanism underlying this refractive index modification gives rise to an anisotropy. This phenomenon has been reported in several works (Yang et al., 2004; Jovanovic et al., 2009; Wang et al., 2023) that used different experimental conditions such as laser energy; numerical aperture (NA) of focusing lenses (microscope objectives), repetition rate and scanning speed. Despite the disparity in the inscription parameters which gave rise to different birefringence values, it comes out that the polarization of the laser beam has a major influence on the axes of the induced birefringence (Ams et al., 2006). Moreover; with increasing laser energy and exposure time or scanning speed the refractive index modification can go through different regimes: an increase, or even a saturation effect followed by a decrease in the areas of material with void formation (Jovanovic et al., 2009). Furthermore; it has been demonstrated that when the repetition rate of the fs laser pulses exceeds 500 kHz (Eaton et al., 2008); thermal-heating effect occurs due to a cumulative regime that homogeneously impacts the medium, thereby counteracting the birefringence effect.

In this work, we study the optical properties of a multi-scan waveguide inscribed with relatively low energy (130 nJ), high repetition rate (1 MHz) and very low scanning speed (0.25 mm/s). To probe and check the induced birefringence, we inscribed a grating in the waveguide. First of all, relying on a transmission optical microscope, we studied the shape of the engineered waveguide in its cross-section. With Digital Holographic Microscopy (DHM), we were able to evaluate the refractive index modification induced in the waveguide with respect to non-engineered substrate and retrieve the numerical aperture (NA) of the waveguide. This was performed as a function of the pulse energy between 130 and 200 nJ. In exploring this aspect, our attention turned towards evaluating the photo-induced birefringence associated with the fabrication of both the waveguide and Bragg grating. The quantification of the latter derived from polarization-dependent measurements of the grating spectrum in reflection mode. This analysis supports the correlation between birefringence and the polarization state of the femtosecond laser interacting with the glass substrate. Significantly, we observed minimal birefringence when the writing laser beam was linearly polarized along the direction of the sample scanning, aligning with the findings of previous relevant work (Ams et al., 2006). This work brings interesting highlights about the femtosecond laser engineering process in glass and allows to further optimize the design of such structures. The study of birefringence effects opens the way to future transverse strain measurements; as already performed in fiber Bragg gratings (Caucheteur et al., 2007).

2. Experiments

The FemtoPrint device was used to create the optical waveguides and the in-built Bragg gratings in planar glass substrates. Fig. 1 shows a picture of the set-up together with a sketch of the manufacturing process. The FemtoPrint encompasses a Satsuma SY-4234 SHG 1030 nm laser, a fixed microscope objective (LMH-20x-1064 from Thorlabs, NA = 0.4) and a three-axis translation stage. The focused laser pulses are characterized by a voxel of 24 μm x 3 μm and are delivered with a repetition rate of 1 MHz and a pulse duration of 200 fs. Their energy can be adjusted to yield different types of modification, as discussed in the introductory part.

Using this device, similar structures as the ones reported in (Amezdroz et al., 2023; Tunon de Lara et al., 2022) were implemented and used in this work; while another equipment was used for their characterization. For the observation of the waveguide, we used an optical microscope from Zeiss, an Axio imager.M2. In the framework of this study, this microscope is only used for the quantitative analysis and basic observations such as size measurements, whereas the Digital Holographic Microscopy (DHM) is used to measure the modification of the refractive index. DHM uses laser light to create interference patterns when it interacts with a specimen. These interference patterns are recorded as a digital hologram and then numerically reconstructed on a computer to produce a high-resolution 3D image of the specimen. DHM offer the advantage of capturing both amplitude and phase information, making them valuable in various fields, including biology and materials science, where precise 3D imaging is crucial. To study birefringence effects, the substrates were connected to a single-mode optical fiber and the grating spectra were measured in reflection mode using a broadband optical source (Amonics ALS-CL-17-B-FA), a circulator and an optical spectrum analyzer (Yokogawa AQ6374D), as sketched in Fig. 2. A polarizer and a polarization controller were used in the path between the source and the circulator to modify the input polarization state and study its effect on the reflected amplitude spectrum.

In the following section, we present and discuss the different experimental results obtained following the characterizations performed in this study.

3. Experimental results

The femtosecond laser generates pulses at a repetition rate of 1 MHz with 200 fs pulse duration. To achieve a uniform and consistent waveguide with an even distribution of the refractive index, we chose to use a technique of several overlapping laser scanning lines (multiple parallel passages). Each path overlaps with the others to form a homogeneous structure. This technique allows a better control of the cross-sectional size of the waveguide. Despite the provided voxel size by the Femtoprint supplier (3 μm × 24 μm), we have measured the size of the refractive index modification induced in our fused silica substrate by an optical transmission microscope (Zeiss Axio imager.M2). We noticed that for 130nJ pulse energy focused though 0.40NA microscope objective, the modified area in the substrate does not exceed 2 μm × 12 μm. Therefore, to keep a square-like shape waveguide cross-section and for better matching of the core diameter of a standard single mode optical fiber, we choose a multi-scan along the z direction to reach 10 μm width. In the current scenario, we have used very low scanning speed of 0.25 mm/s along the substrate (z axis) for high overlapping of the voxels and 16 parallel passages, spaced by 0.5 μm (Tunon de Lara et al., 2022). Fig. 3 represents two types of views observed with the optical microscope to characterize the morphology of the waveguide. It is interesting

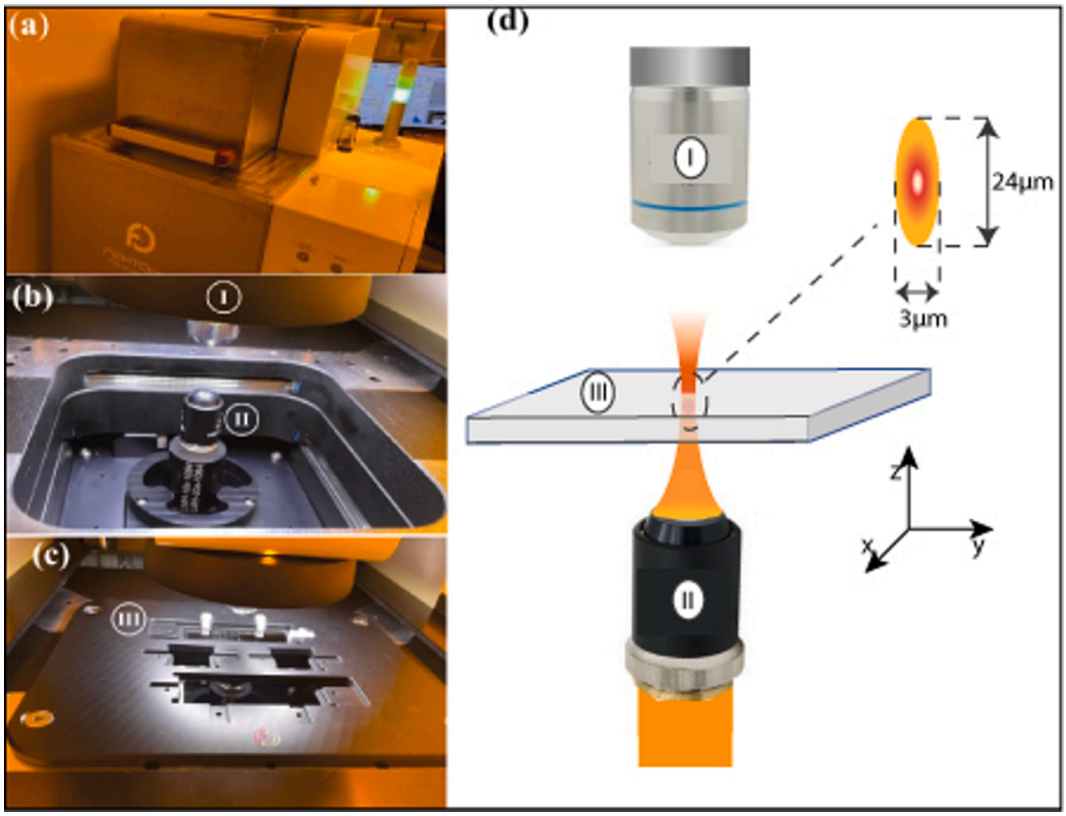

Fig. 1. **(a)** Picture of the Femtoprint machine installed in our clean room **(b)** Picture of the inside of the Femtoprint machine showing the microscope objective (I) used for the visualization process and the other objective used to focus the femtosecond laser pulses (II). **(c)** Picture of the moving plate of the Femtoprint machine containing a glass substrate set for printing (III). **(d)** Schematic representation of the Femtoprint process.

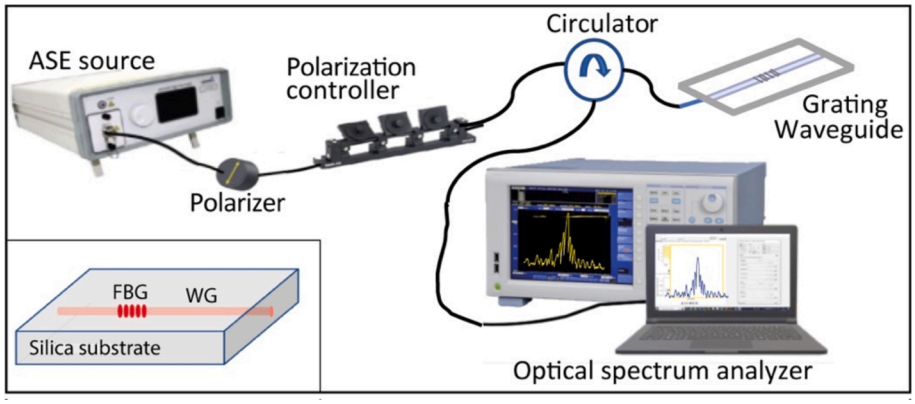

Fig. 2. Schematic representation of the optical fiber set-up used to characterize the grating birefringence in reflection mode using a broadband amplified spontaneous emission (ASE) optical source, a polarizer, polarization controller and an optical spectrum analyzer. Inset: a close-up sketch of the grating waveguide.

to note that the transmission microscope image of the glass plate shows a homogeneous waveguide structure of 10 µm in diameter; while the cross-section transmission microscope images reveal a quasi-square shape with lines and areas of different contrasts under polarized light. These observations indicate the stress built-up in the fused silica due to the material migration after the creation of micro-holes. It is therefore relevant to investigate the photo-induced birefringence of such structure, as we will do in the following.

Existing literature suggests that low-energy femtosecond laser pulses induce densification in the silica glass by altering the structure of Si-O bonds, resulting in variations in refractive index represented in Fig. 4 (Taylor et al., 2003; Chan et al., 2001). The densification of SiO_2 arises from a change in the dimensions of the rings before exposure to a femtosecond laser. Initially; there exists a variety of ring sizes. However, upon irradiation process, the rings undergo a reduction in size, leading to a densification effect.

This densification is observable with the DHM due to the interference and phase changes it causes. Fig. 5 illustrates the waveguide's refractive index evolution as a function of the pulse energy used for inscribing the optical structure. Our objective was to establish a relationship between pulse energy and refractive index evolution. It is worth to mention that despite the relatively high repetition rate of the laser beam (1 MHz), this relationship is linear and does not show a saturation limit. However, when using pulses energy higher than 170 nJ the standard deviation is higher. This observation is probably due to an increase of micro-holes with increased energy and a non-uniform distribution of the refractive

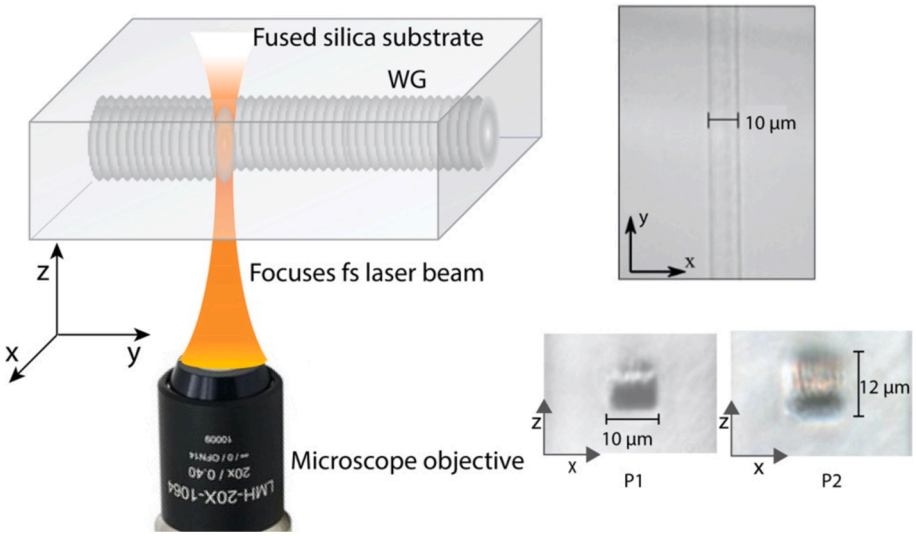

Fig. 3. Sketch of the femtosecond laser patterning process for waveguide creation in planar substrate, with transmission optical microscope pictures showing top view and the cross section of the waveguide under different polarization of the light P1 and P2. We can see the stress arears generating different birefringences along the inscription direction.

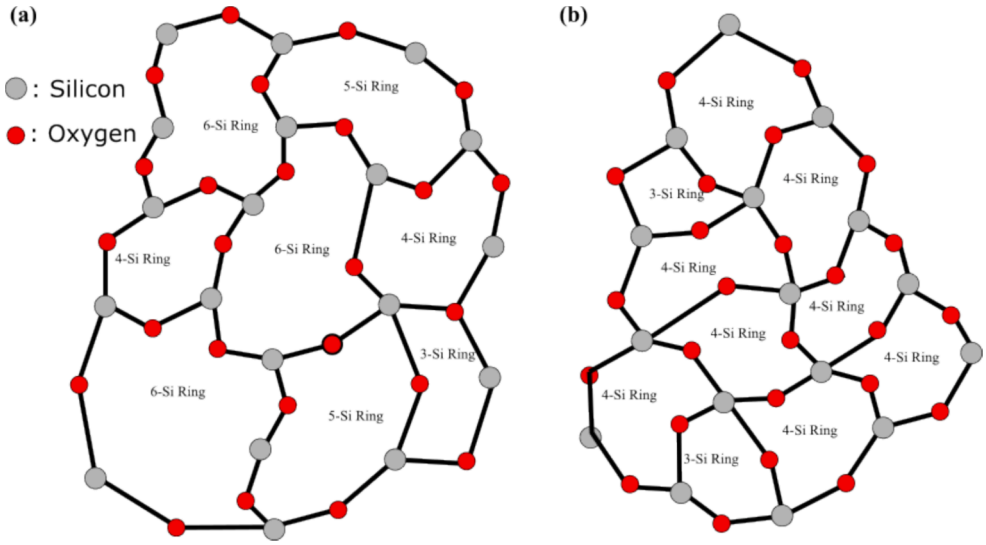

Fig. 4. Schematic representation of the fused silica structure: **(a)** pristine and **(b)** after its irradiation by a femtosecond laser at low energy.

index change. This latter can either increase dramatically or decrease. In the case of our experiments we obtained a dispersion between the characterized samples which may be a consequence of the threshold of the high energy regime.

In light of the previous refractive index measurements by means of DHM, we have derived the values of the NA of the optical waveguides according to the following equation:

$$NA = \sqrt{{n_1}^2 - {n_2}^2} \tag{1}$$

Where n_1 and n_2 are the refractive indices of the modified and unmodified silica substrate respectively. Considering the refractive index of the silica glass at 1500 nm to be 1.44462, according to the manufacturer's datasheet, and as 1.44739 based on DHM measurements for the waveguide produced with 130 nJ pulse energy, we determine the corresponding NA to be 0.09. This value suggests that the propagation of light in our waveguide is single-mode, which is also confirmed by the fact that the reflected amplitude spectrum of the in-built Bragg grating displays only a single main resonance. Besides, we used the experimental setup depicted in Fig. 6 to determine experimentally the NA of the waveguide. We couple an HeNe laser source (632.8 nm) in the waveguide and measure the light distribution at its output with a detector equipped with a slit of 1 mm width. The following formula is used once the acceptance angle θ is determined.

$$NA = n\sin\theta \tag{2}$$

To do so, we positioned the detector at 10 cm away from the waveguide output and displace it perpendicularly to the laser beam direction until the measured power drops to 5 % from the maximum value. The NA was determined to be 0.08. This value is comparable to the one retrieved from DHM analysis.

To capture the near-field intensity distribution, the output light from the waveguide is imaged using a microscope objective and a CCD camera (Fig. 7). A gaussian profile is used for the analysis in both directions (x and y). The typical diameter of the mode field is approximately 10 µm. From the inset of Fig. 7, we show the high symmetry of the near-field distribution despite the possible non-circular shape of the

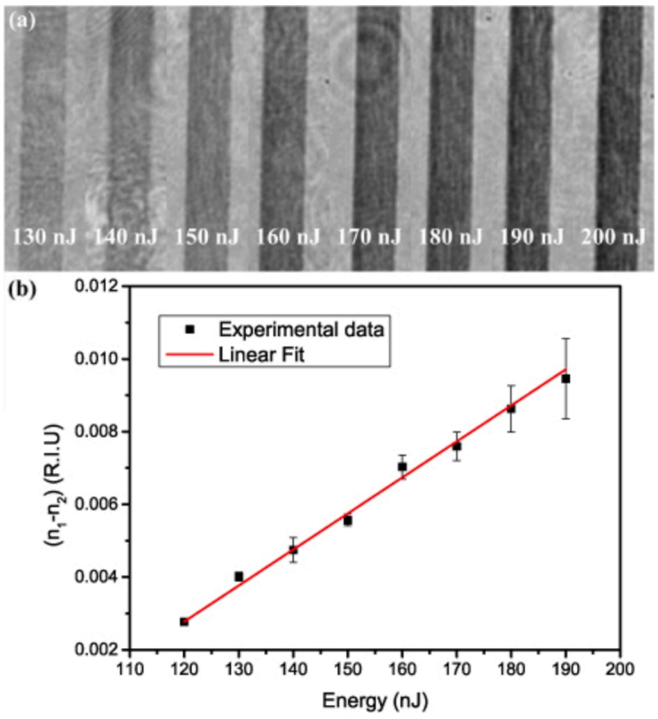

Fig. 5. DHM pictures of the waveguides for different laser pulse energies (from 130 nJ to 200 nJ by steps of 10 nJ) **(a)** and refractive index increase (n_1-n_2) of the waveguide as a function of the pulse energy (n_1 and n_2 are the modified and unmodified substrate's refractive indices respectively). The standard deviation is obtained from three measurements **(b)**.

cross-section of the waveguide shown previously in Fig. 3.

After characterizing the properties of the waveguide, our next investigative phase is the inscription of a Bragg grating. A Bragg grating is a periodic structure (Λ) of a certain length (L) that reflects specific wavelengths (λ_{BG}) of light while allowing others to pass through. This Bragg grating was inscribed during the same operational procedure as the waveguide. The inscription process consists in multi-scan of the cross section of the waveguide with the laser beam. The uniform period between the scanned lines is $\Lambda = 1.1$ μm for a total length of the grating L = 3 mm, as reported in (Tunon de Lara et al., 2023). Our analysis focused on the second-order Bragg peak positioned at 1588 nm. We relied on polarized light to scrutinize the ensuing impact of birefringence on the optical response. In doing so; we made a noteworthy observation: the Bragg peak exhibited a discernible spectral shift depending on the input polarization state. This shift is a direct consequence of the photo-induced birefringence during the manufacturing process, a phenomenon spectrally represented in Fig. 8 for the two input states of polarization that yield the maximum wavelength separation between the reflected amplitudes. This corresponds to the so-called fast axis (blue curve) and slow axis (red curve). Hence, this birefringence is manifested as a differential shift of 300 pm in the maximum reflection wavelength (wavelength separation between the blue and red curves of Fig. 8). This experimental outcome underscores the influence of waveguide-induced birefringence on the spectral characteristics of the Bragg grating. It is known that, for Bragg gratings, the wavelength separation between the slow and fast axes corresponds to $\Delta n.\Lambda$ for a second order grating where Δn is the birefringence value and Λ the grating period (Caucheteur et al., 2007). Hence; a wavelength separation of 300 pm corresponds to a birefringence value of 2.7 10^{-4}. This birefringence corresponds to typical values reached in polarization maintaining optical fibers. The main impacting factors of the birefringence value are the asymmetric shape of

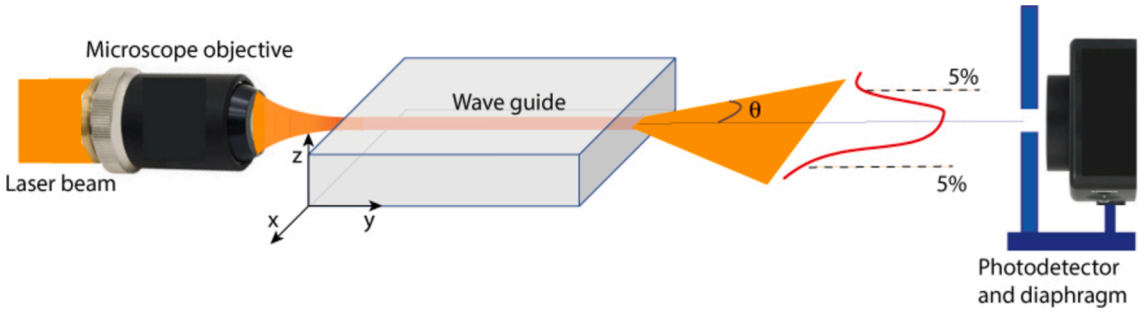

Fig. 6. Sketch of the experimental setup for numerical aperture (NA) determination.

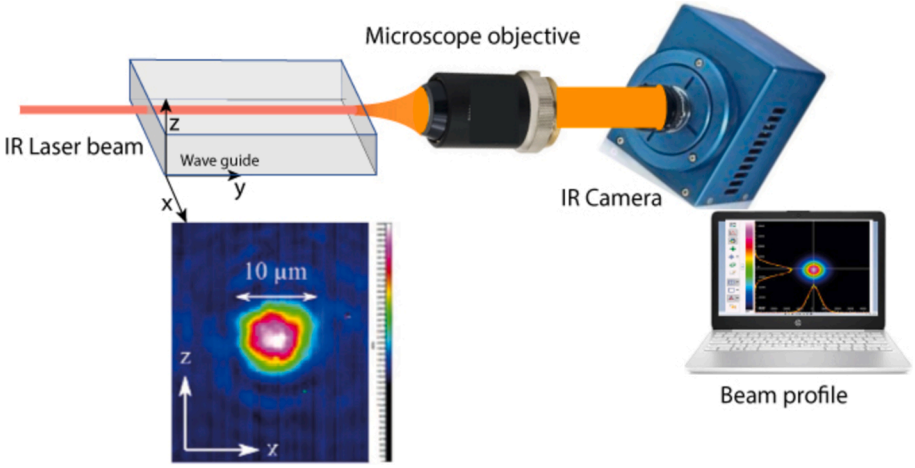

Fig. 7. Experimental setup for mode field diameter and near-field intensity distribution measurements.

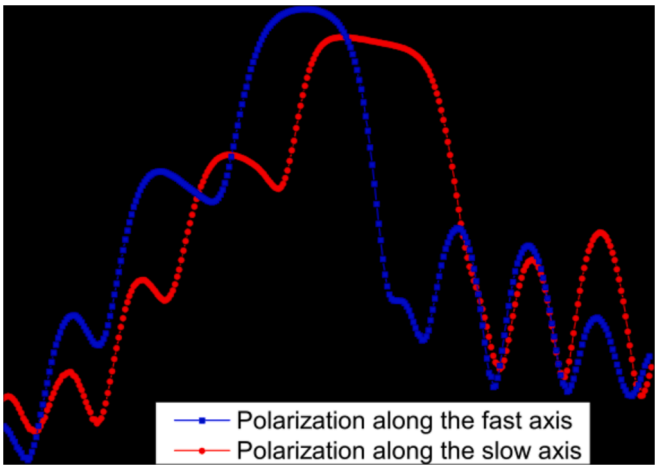

Fig. 8. Reflected amplitude spectrum of the Bragg grating measured for two orthogonal polarization states (x and z).

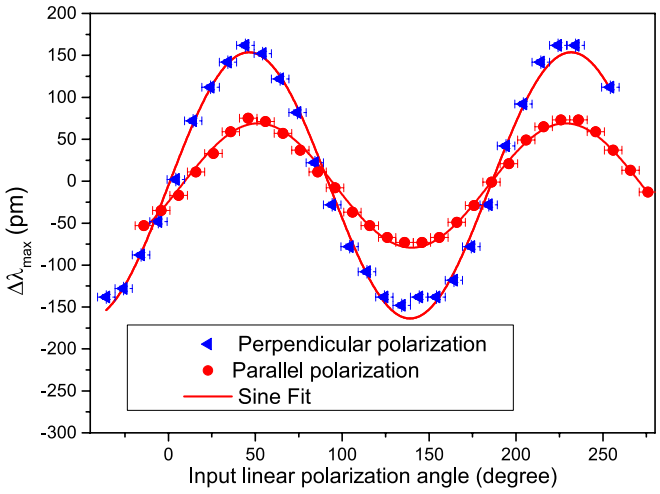

Fig. 9. Schematic representation and characterization curve of the evolution of the Bragg wavelength as a function of the state of polarization in the case of a waveguide inscribed with a perpendicular polarized inscription **(a)** and parallel polarized inscription **(b)**.

the waveguide cross-section and/or the induces stress in the surrounding structures formed during the writing process. As stated previously, a special attention was paid to produce a waveguide with symmetrical cross-section. However, despite the high repetition rate (1 MHz) which may create thermal-heating effect (Eaton et al., 2008); we noticed at low scanning speed (0.25 mm/s) and relatively low pulses energy (130nJ) an inbuilt stress in the waveguide as shown in Fig. 3. A better control and tuning of the induced-birefringence can be performed by controlling the laser polarization and pulse energy during the writing process (Wang et al., 2023). We therefore investigate the effect of the inscription laser polarization state on the photo-induced birefringence.

To this end, we conducted reflective measurements on two waveguides inscribed under parallel and perpendicular polarization respectively with respect to the laser scanning direction. The other inscription parameters were kept the same such that the pulse energy (130 nJ), the translation speed (0.25 mm/s) and the repetition rate (1 MHz). The Bragg grating shared identical inscription parameters with the waveguide except the pulse energy which was increased to 150 nJ. The inscription method for the grating is Line-by-Line scanning the cross section of the waveguide with 1.1 μm period between the lines. Subsequently, we characterized the evolution of birefringence by measuring the reflection spectrum of the Bragg grating under different angles of the input linear polarization of the light with an increment of ten degree. The primary objective of this investigation was to derive a comprehensive and nuanced understanding of birefringence evolution in response to varying degrees of polarization.

A significant difference between the two characterizations can be seen in Fig. 9. The curve with blue triangles corresponds to the measurements for the waveguide inscribed using perpendicular-polarized femtosecond laser beam, whereas the red circles are the data of the waveguide inscribed with parallel-polarized femtosecond laser light. For the parallel laser polarization, the wavelength separation linked to the birefringence drops to 142 pm, corresponding to a birefringence value of $1.3\ 10^{-4}$.

These observations confirm that the utilization of perpendicular-polarized and parallel-polarized femtosecond laser light imparts a unique birefringence to the waveguides, giving rise to distinct optical properties and behaviors. Indeed, the process of writing is the result of the interaction of the femtosecond pulses with the used material, in this case fused silica. The underlying physical mechanisms such as multi-photon ionization, avalanche effect and other nonlinear effects are highly dependent on the polarization of the light wave (Little et al., 2008; Tan et al., 2016). Therefore; it is clear that the change in the material refractive index will be impacted by the polarization of the laser beam. The observed divergence in polarization orientation offers a valuable avenue for exploring and understanding the waveguide's response to different polarizations and opens up opportunities for tailored applications in optical communication and photonic devices (Tan et al., 2016). This phenomenon underscores the precise control over the polarization characteristics during the fabrication process; highlighting the potential for customized birefringence in waveguide design. In sensing, it also opens the way to transverse force measurements, as done in (Chah et al., 2013; Caucheteur et al., 2007) for optical fibers for instance.

4. Conclusions

In conclusion, our study has focused on the fabrication and comprehensive characterization of femtosecond laser-inscribed waveguides in silica glass. Such a characterization, both in terms of refractive index modulation and birefringence, is essential towards the production of high-quality structures and we have provided insightful methodologies to achieve this, which we believe will be useful to the scientific community for future advanced manufacturing.

Our findings have not only expanded our understanding of the intricacies of femtosecond laser-inscribed waveguides but have also opened new avenues for tailored applications in the field of optics and photonics. The ability to control birefringence in such waveguides represents a significant step forward, with potential implications for advanced optical communication systems, signal processing, and photonic device development. As a testament to the versatility and precision of femtosecond laser technology, our work has contributed to the growing body of knowledge in this area and encourages further exploration of the potential applications and optimizations in waveguide-based optical systems. Future research can focus on refining the control and manipulation of birefringence to harness the full potential of these waveguides in various technological domains.

CRediT authorship contribution statement

M.Tunon de Lara: Writing – review & editing, Writing – original draft, Methodology, Investigation, Conceptualization. **L.Amez Droz:** Writing – review & editing, Validation, Investigation. **K. Chah:** Writing – review & editing, Validation, Supervision, Formal analysis, Data curation. **P. Lambert:** Writing – review & editing, Validation, Supervision, Project administration, Methodology, Funding acquisition, Conceptualization. **C. Collette:** Writing – review & editing. **C.**

Caucheteur: Writing – review & editing, Supervision, Project administration, Conceptualization.

Declaration of competing interest

The authors declare that they have no known competing financial interests or personal relationships that could have appeared to influence the work reported in this paper.

Acknowledgement

The authors gratefully acknowledge the "Fonds de la Recherche Scientifique", Research project grant INFuSE (grant agreement number FNRS PDR T.0049.20), for funding this research.

Funding's

"Fonds de la Recherche Scientifique", Research project grant INFuSE (grant agreement number FNRS PDR T.0049.20).

Data availability

Data will be made available on request.

References

Amez-droz, L., De Lara, M.T., Collette, C., Caucheteur, C., Lambert, P., 2023. Instrumented Flexible Glass Structure: A Bragg Grating Inscribed with Femtosecond Laser Used as a Bending Sensor. Sensors 23 (19), 8018. https://doi.org/10.3390/s23198018.

Ams, M., Marshall, G.D., Withford, M.J., 2006. Study of the influence of femtosecond laser polarisation on direct writing of waveguides. Opt. Express. 14, 13158. https://doi.org/10.1364/oe.14.013158.

Bellouard, Y., 2011. On the bending strength of fused silica flexures fabricated by ultrafast lasers. Opt. Mater. Express. 1, 816. https://doi.org/10.1364/ome.1.000816.

Bellouard, Y., Said, A., Dugan, M., Bado, P., 2004. Fabrication of high-aspect ratio, micro-fluidic channels and tunnels using femtosecond laser pulses and chemical etching. Opt. Express. 12, 2120. https://doi.org/10.1364/opex.12.002120.

Beresna, M., Gecevičius, M., Kazansky, P.G., 2014. Ultrafast laser direct writing and nanostructuring in transparent materials. Adv. Opt. Photonics. 6, 293. https://doi.org/10.1364/aop.6.000293.

Canning, J., Lancry, M., Cook, K., Weickman, A., Brisset, F., Poumellec, B., 2011. Anatomy of a Femtosecond Laser Processed Silica Waveguide 1, 998–1008.

Casamenti, E., Pollonghini, S., Bellouard, Y., 2021. Few pulses femtosecond laser exposure for high efficiency 3D glass micromachining. Opt. Express. 29, 35054. https://doi.org/10.1364/oe.435163.

Caucheteur, C., Bette, S., Garcia-Olcina, R., Wuilpart, M., Sales, S., Capmany, J., Mégret, P., 2007. Transverse strain measurements using the birefringence effect in fiber Bragg gratings. IEEE Photonics Technol. Lett. 19, 966–968. https://doi.org/10.1109/LPT.2007.897566.

Chah, K., Kinet, D., Wuilpart, M., Mégret, P., Caucheteur, C., 2013. Femtosecond-laser-induced highly birefringent Bragg gratings in standard optical fiber. Opt. Lett. 38, 594. https://doi.org/10.1364/ol.38.000594.

Chan, J.W., Huser, T., Risbud, S., Krol, D.M., 2001. Structural changes in fused silica after exposure to focused femtosecond laser pulses. Opt. Lett. 26, 1726. https://doi.org/10.1364/ol.26.001726.

Eaton, S.M., Zhang, H., Ng, M.L., Li, J., Chen, W.J., Ho, S., Herman, P.R., 2008. Transition from thermal diffusion to heat accumulation in high repetition rate femtosecond laser writing of buried optical waveguides. Opt. Express 16, 9443–9458. https://doi.org/10.1364/OE.16.009443.

Gattass, R.R., Rafael, R., Mazur, E., 2008. Femtosecond laser micromachining in transparent materials. Nat. Photonics 2 (4), 219–225. https://doi.org/10.1038/nphoton.2008.47.

Hnatovsky, C., Taylor, R.S., Rajeev, P.P., Simova, E., Bhardwaj, V.R., Rayner, D.M., Corkum, P.B., 2005. Pulse duration dependence of femtosecond-laser-fabricated nanogratings in fused silica. Appl. Phys. Lett. 87. https://doi.org/10.1063/1.1991991.

Joglekar, A.P., Liu, H., Spooner, G.J., Meyhöfer, E., Mourou, G., Hunt, A.J., 2003. A study of the deterministic character of optical damage by femtosecond laser pulses and applications to nanomachining. Appl. Phys. B Lasers Opt. 77, 25–30. https://doi.org/10.1007/s00340-003-1246-z.

Jovanovic, N., Thomas, J., Williams, R.J., Steel, M.J., Marshall, G.D., Fuerbach, A., Nolte, S., Tünnermann, A., Withford, M.J., 2009. Polarization-dependent effects in point-by-point fiber Bragg gratings enable simple, linearly polarized fiber lasers. Opt. Express 17, 6082–6095.

Kiyama, S., Matsuo, S., Hashimoto, S., Morihira, Y., 2009. Examination of etching agent and etching mechanism on femotosecond laser microfabrication of channels inside vitreous silica substrates. J. Phys. Chem. c. 113, 11560–11566. https://doi.org/10.1021/jp900915r.

Li, L., Kong, W., Chen, F., 2022. Femtosecond laser-inscribed optical waveguides in dielectric crystals: a concise review and recent advances. Advanced Photonics 4, 2. https://doi.org/10.1117/1.AP.4.2.024002.

Little, D.J., Ams, M., Dekker, P., Marshall, G.D., Dawes, J.M., Withford, M.J., 2008. Femtosecond laser modification of fused silica: the effect of writing polarization on Si-O ring structure. Opt. Express 16, 20029–20037. https://doi.org/10.1364/OE.16.020029.

Liu, X., Du, D., Mourou, G., 1997. Laser ablation and micromachining with ultrashort laser pulses. IEEE J. Quantum Electron. 33, 1706–1716. https://doi.org/10.1109/3.631270.

Malinauskas, M., Žukauskas, A., Hasegawa, S., Hayasaki, Y., Mizeikis, V., Buividas, R., Juodkazis, S., 2016. Ultrafast laser processing of materials: From science to industry. Light Sci. Appl. 5, 3–5. https://doi.org/10.1038/lsa.2016.133.

Marcinkevičius, A., Juodkazis, S., Watanabe, M., Miwa, M., Matsuo, S., Misawa, H., Nishii, J., 2001. Femtosecond laser-assisted three-dimensional microfabrication in silica. Opt. Lett. 26, 277. https://doi.org/10.1364/ol.26.000277.

Pasaila, N.D., Thomson, R.R., Bookey, H.T., Kar, A.K., Chiodo, N., Osellame, R., Cerullo, G., Brown, G., Jha, A., Shen, S., 2006. Femtosecond laser inscription of optical waveguides in Busmuth ion doped glass. Opt. Express. 14 (22), 10452–10459.

Tan, D., Sharafudeen, K.N., Yue, Y., Qiu, J., 2016. Femtosecond laser induced phenomena in transparent solid materials: Fundamentals and applications. Prog. Mater Sci. 76, 154–228. https://doi.org/10.1016/j.pmatsci.2015.09.002.

Taylor, R.S., Hnatovsky, C., Simova, E., Rayner, D.M., Bhardwaj, V.R., Corkum, P.B., 2003. Ultra-high resolution index of refraction profiles of femtosecond laser modified silica structures. OSA Trends Opt. Photonics Ser. 88, 1248–1249. https://doi.org/10.1364/oe.11.000775.

Taylor, R.S., Hnatovsky, C., Simova, E., Rayner, D.M., Bhardwaj, V.R., Corkum, P.B., 2003. Femtosecond laser fabricated nanostructures in silica glass. OSA Trends Opt. Photonics Ser. 88, 1009–1010. https://doi.org/10.1364/ol.28.001043.

Tien, A.C., Backus, S., Kapteyn, H., Murnane, M., Mourou, G., 1999. Short-pulse laser damage in transparent materials as a function of pulse duration. PhysRevLett. 82, 3883–3886. https://doi.org/10.1103/PhysRevLett.82.3883.

Tunon de Lara, M., Chah, K., Amez-Droz, L., Lambert, P., Collette, C., Caucheteur, C., 2022. Production of an optical waveguide in planar glass substrate fabricated with femtoprint. Proc. SPIE. International Society for Optical Engineering, Bellingham, USA.

Tunon de Lara, M., Amez-Droz, L., Chah, K., Lambert, P., Collette, C., Caucheteur, C., 2023. Femtosecond pulse laser-engineered glass flexible structures instrumented with an in-built Bragg grating sensor. Opt. Express. 31, 29730. https://doi.org/10.1364/oe.497482.

Wang, Y.D., Li, Z.Z., Li, Y.C., Duan, Y.Z., Wang, L.C., Yu, Y.H., Chen, Q.D., 2023. Ultralow birefringent glass waveguide fabricated by femtosecond laser direct writing. Opt. Letters 48 (3), 554–557.

Wang, X., Yu, H., Li, P., Zhang, Y., Wen, Y., Qiu, Y., Liu, Z., Li, Y.P., Liu, L., 2021. Femtosecond laser-based processing methods and their applications in optical device manufacturing: A review. Opt. Laser Technol. 135, 106687. https://doi.org/10.1016/j.optlastec.2020.106687.

Will, M., Nolte, S., Chichkov, B.N., Tünnermann, A., 2002. Optical properties of waveguides fabricated in fused silica by femtosecond laser pulses. Appl. Opt. 41 (21), 4360–4364. https://doi.org/10.1364/AO.41.004360.

Yang, P., Burns, G.R., Guo, J., Luk, T.S., Vawter, G.A., 2004. Femtosecond laser-pulse-induced birefringence in optically isotropic glass. J. Appl. Phys. 95, 5280. https://doi.org/10.1063/1.1707231.

Zhou, K., Dubov, M., Mou, C., Zhang, L., Mezentsev, V.K., Bennion, I., 2010. Line-by-line fiber bragg grating made by femtosecond laser. IEEE Photonics Technol. Lett. 22, 1190–1192. https://doi.org/10.1109/LPT.2010.2050877.